

# Improved Pressure Response with Embedded Solid Microbeads in Microfluidic Soft Sensors

Hee-Sup Shin<sup>1</sup> and Yong-Lae Park<sup>1,2</sup>

<sup>1</sup>Mechanical Engineering, Carnegie Mellon University, Pittsburgh, PA 15213, USA.

<sup>2</sup>Robotics Institute, Carnegie Mellon University, Pittsburgh PA 15213, USA

E-mail: heesups@andrew.cmu.edu, ylpark@cs.cmu.edu

**Abstract**—Soft sensors with embedded microchannels filled with liquid conductors have recently been proposed for detecting various types of mechanical stimuli, such as contact pressures, shear forces, strains, and curvatures. Their sensing behaviors are mainly determined by geometrical changes of the embedded microchannels, which is caused by mechanical deformation of the soft structures. In order to control the cross-sectional changes of the microchannels for desired sensor responses, we propose to add solid non-conductive microbeads in the microchannels. Using finite element analysis, we evaluated the influence of the embedded microbeads on the pressure response of soft sensors. We also experimentally compared the pressure responses of soft sensors with rectangular microchannels by changing the number of the beads. Our preliminary results from simulation and experiments showed that the embedded microbeads improved the pressure response of the soft sensors in terms of their linearity, sensitivity, and dynamic range.

## I. INTRODUCTION

Elastomer-based hyperelastic electronics with embedded liquid-phase metal present mechanically and electronically distinct characteristics, which enable transducers for strain, pressure, and forces, and circuits to be flexible, stretchable, and compressible. These soft electronics typically composed of a thin layer of elastomer (e.g. polydimethylsiloxane – PDMS or silicone rubber) with embedded microchannels filled with liquid conductors (i.e. liquid-phase metal alloy) can remain functional when stretched to several times from their original length while maintaining the natural mechanics of the host system. Their properties of mechanical robustness and the electrical simplicity have introduced various types of soft sensors and electronics, such as stretchable electric wires [1], hyperelastic strain sensors [2], [3], pressure sensors [4], [5], multi-axis force sensors [6], [7], curvature sensors for flexible structures [8], wearable electronics and sensors [9], [10], stretchable radio frequency (RF) electronics [11], tactile sensing for micro manipulation [12] and a flexible telemetry system [13].

Since the deformation of surrounding elastomer has a dominant effect on the electrical conductivity of embedded microfluidic channels, the change of the electrical resistance of the microchannels for detecting various modalities is dependent on the elastic deformation of the elastomer. In pressure sensing, an applied pressure will result in the decrease in the cross-sectional area of the embedded microchannels, which consequently increases the electrical resistance of the

microchannels. Therefore, the relationship between the resistance change and the applied pressure is highly influenced by the deformed cross-sectional geometry. Previous research has shown that the pressure response can be significantly improved by changing the cross-sectional geometries of the microchannels [14], [15]. However, the suggested concave triangular microchannels require a complicated and expensive manufacturing process, such as micro-milling machining, compared to typical rectangular microchannels. Furthermore, the narrow corners of the microchannel require sharp and fragile edges in the mold, which are not reliable for multiple sensor replications, even though the mold can be made of hard materials.

In this paper, we introduce solid non-conductive microbeads to be embedded with a liquid conductor in a microchannel to create a similar effect of a concave triangular channel. By adding microbeads in a rectangular microchannel, we were able to create concave triangular shaped gaps between the beads and the walls of the microchannels, which are filled with a liquid conductor. Also, the discretized beads maintain the sensor structure still stretchable without disconnecting the soft circuit. This approach allowed us to use one of the simplest manufacturing processes, such as 3D printing, to build the mold for the soft sensors. The microbead embedded soft sensors showed significantly improved pressure responses in both the finite element analysis (FEA) simulations and the experiments.

## II. MATERIALS AND METHODS

Four sensor samples with different microchannel widths were prepared, as shown in Fig. 1. The first two samples have  $500\mu\text{m} \times 500\mu\text{m}$  microchannels, and one of the two samples has a single bead embedded in the cross-section. The other two samples have a  $1\text{mm}$  (width)  $\times 500\mu\text{m}$  (height) microchannels, and one of these two samples has double beads embedded in the cross-section. The remaining space in the microchannels in both samples were completely filled with a highly conductive liquid metal (eutectic gallium indium – eGaIn). Each microchannel was embedded in a  $50\text{mm}$  by  $100\text{mm}$  rectangular elastomer sheet (EcoFlex 0030; Smooth-On) that is  $10\text{mm}$  thick. Fig. 2 shows the actual microbeads embedded in different sized microchannels.

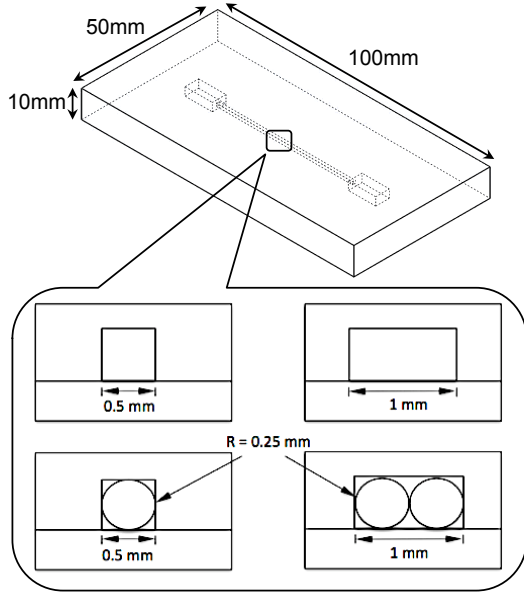


Fig. 1. Pressure sensor sample designs with different channel dimensions. The top two channels in the callout are empty and the other two channels have embedded microbeads.

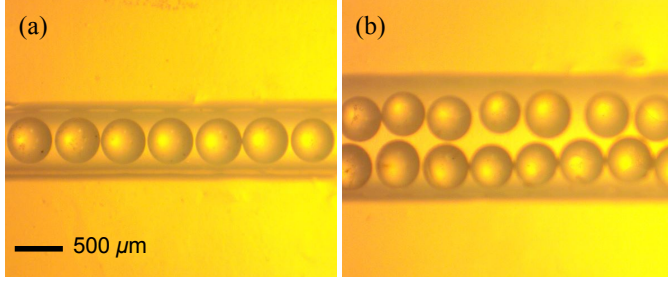


Fig. 2. Microscopic top views of microbead embedded samples. (a)  $500\mu\text{m}$  width microchannel with a single microbead in the cross-section. (b)  $1\text{mm}$  width microchannel with double microbeads in the cross-section.

Each sample is fabricated by casting two silicone layers – a flat top layer and a microchannel patterned bottom layer – in rigid plastic molds made with a 3D printer (Objet30, Stratasys). Once the two layers are cured, microbeads are poured into the microchannel through the open top of the channel. The excessive beads are removed using a sticky cellophane tape. Manual alignment of the microbeads are sometimes necessary to fill any empty space. Then, the top layer is bonded to close the open top of the microchannel. Finally eGaIn is injected from one end of the microchannel using a hypodermic needle. More details on fabrication of eGaIn microchannel embedded soft sensors can be found in the previous work [2], [4].

### III. RESULTS

#### A. Simulation

A series of a two-dimensional plane-strain simulation were implemented by the commercial FEA software pack-

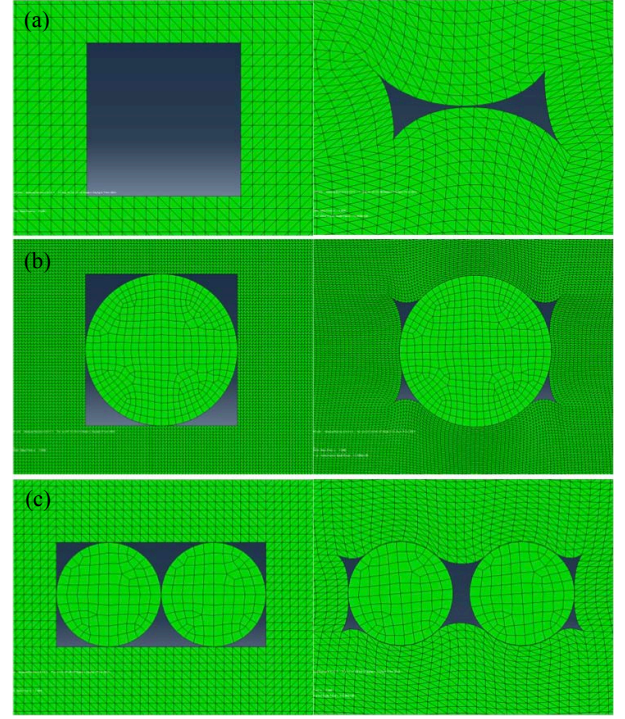


Fig. 3. Simulation models showing initial and final microchannel shapes. (a) Empty channel ( $500\mu\text{m} \times 500\mu\text{m}$ ). (b) Single bead embedded channel ( $500\mu\text{m} \times 500\mu\text{m}$ ). (c) Double bead embedded channel ( $1\text{mm} \times 500\mu\text{m}$ )

age (ABAQUS/CAE 6.13-3, Dassault Systemes) to predict the geometrical deformation of an incompressible silicone rubber ( $E=125\text{ kPa}$  and  $\nu=0.49$  [4]) affected by embedded solid microbeads ( $E=72\text{ GPa}$  and  $\nu=0.22$ ). For the boundary and loading conditions, the bottom of the sensors was fixed (encastre) and a pressure was applied on the top surface with a fixed width ( $15\text{ mm}$ ). The magnitude of the applied pressure was linearly increased from  $0\text{ kPa}$  to  $70\text{ kPa}$ . Frictionless contact conditions were applied to the channel walls for self-contact and between the channel walls and the microbead surfaces. During the simulation, the silicone rubber was assumed to be a homogeneous and isotropic Neo-Hookean solid, and the coefficients of Neo-Hookean model,  $C_{10}$  and  $D_1$  in ABAQUS/CAE [16] were used. The area changes of the microchannels were calculated in a post-process to estimate the electrical resistance changes.

Fig. 3 shows initial and deformed shapes of the cross-sections of the microchannels with different conditions. As expected, the corners of the microchannels with embedded beads deform similar to the shape of a concave triangle. The results are shown in Fig. 4. Although the sensitivity was decreased, the response in bead embedded microchannels were highly linearized. The decreased sensitivity may be due to the increased overall stiffness of the entire structure from the embedded solid elements.

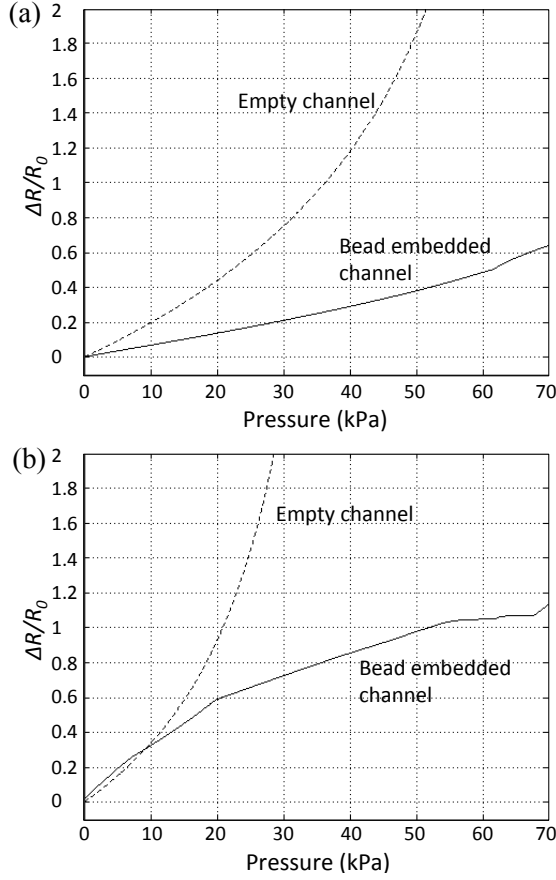


Fig. 4. Simulation Results. (a) Pressure response of an empty microchannel sensor and a single bead embedded sensor. (b) Pressure response of an empty microchannel sensor and a double bead embedded sensor.

### B. Experiments

The prepared samples were tested by applying varied pressures in a constant area (15mm  $\times$  15 mm square) and measuring the electrical resistance of the microchannels. Both empty channels and bead embedded channels were tested, and the results are shown in Fig. 5.

The results show that the linearity of the pressure responses were significantly improved by embedding solid microbeads in the microchannels. Consequently, the minimum detectable pressure and the dynamic range of the sensors were also improved. While the dynamic range of the empty channel sensors is less than 30kPa, that of bead embedded sensors is over 70kPa. Also, while the minimum detectable pressure based on the deviation of the sensor signals is approximately 20kPa with empty channel sensors, the bead embedded sensors are able to detect pressure from approximately 5kPa due to the increased linearity and sensitivity.

The simulation results and the experimental results are highly agreeable in terms of sensitivity, linearity, and output magnitude. The difference of the two results may come from the inaccurate material properties and also elastomer models in the simulation. Also, the initial shapes of the microchannels

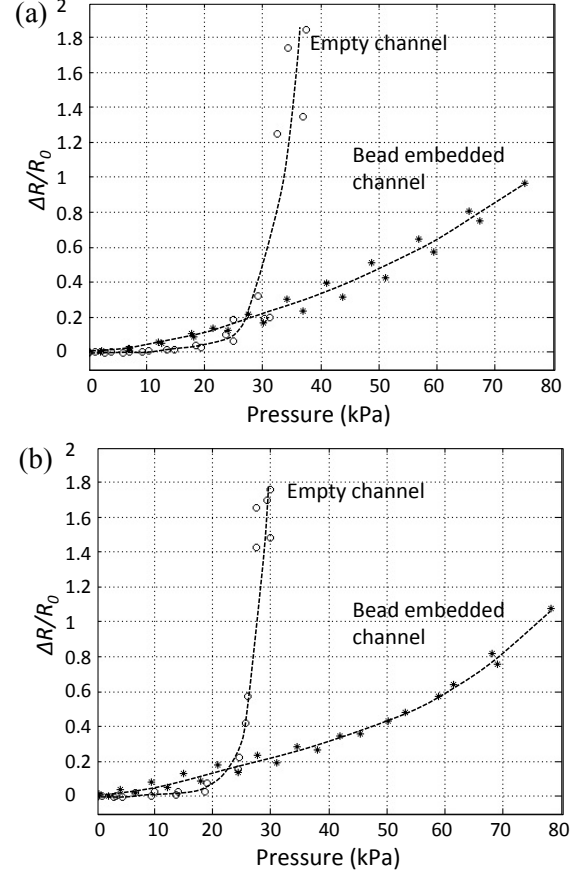


Fig. 5. Experimental Results. (a) Pressure response of an empty microchannel sensor and single bead embedded sensor. (b) Pressure response of an empty microchannel sensor and a double bead embedded sensor.

of the actual prototypes may not be sharp rectangles due to the limited resolution of the 3D printer.

### IV. DISCUSSION

Our results showed that the pressure response of liquid conductor embedded soft sensors can be improved by adding non-conductive solid elements in a conductive microchannel. However, there are several challenges to implement our approach to practical applications. The future work will focus on addressing the following issues.

The diameter of the microbeads used in the experiments varied between 425 $\mu$ m and 500 $\mu$ m. Also, geometrical defects were observed in some beads, which form non-spherical shapes. This nonuniform size and the irregular shapes, shown in Fig. 6, sometimes create undesired empty space between the beads, which may consequently result in less repeatable sensor responses. Using more uniform beads will improve the sensor response to be more reliable.

Although the proposed method does not require a complicated manufacturing process for molds, the manual insertion process of microbeads into a microchannel required extra time and cares. One approach to solve this problem is mixing the microbeads in a liquid conductor. The injection of the

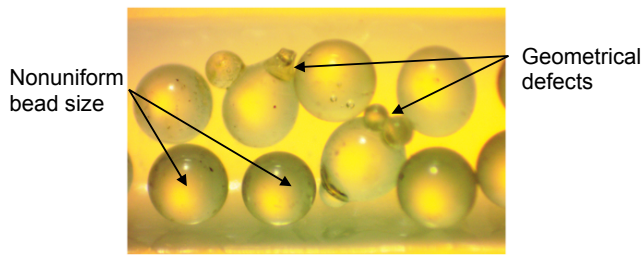


Fig. 6. Inconsistency in the bead geometry.

mixture into a microchannel will allow us to embed the two heterogeneous materials simultaneously in a single process, which further simplifies the fabrication.

The current approach uses only rigid microbeads. However, the mechanical properties of the embedded elements may also affect the sensor response. To maximize the performance of the sensors, it would be useful to consider testing different types of microbeads with different material properties in the future.

## V. CONCLUSION

The main contribution of this work is to propose a simple method to improve the sensor response for pressure sensing by introducing solid microbeads in the embedded microchannel. The proposed approach not only simplifies the manufacturing process but also provide more reliable sensor measurements by linearizing the output signals. The simulation and experiments verified that the addition of microbeads significantly affects the pressure response. Using the proposed method, we were able to generate more linear pressure response. Development of analytical models that can generally predict the deformation of the microbead embedded microchannels is one of our immediate future research areas. Further miniaturization of the sensor using even smaller microbeads is also included in our future work.

## REFERENCES

- [1] M. D. Dickey, R. C. Chiechi, R. J. Larsen, E. A. Weiss, D. A. Weitz, and G. M. Whitesides, "Eutectic gallium-indium (EGaIn): A liquid metal alloy for the formation of stable structures in microchannels at room temperature," *Adv. Funct. Mater.*, vol. 18, no. 7, pp. 1097–1104, 2008.
- [2] Y.-L. Park, B. Chen, and R. J. Wood, "Design and fabrication of soft artificial skin using embedded microchannels and liquid conductors," *IEEE Sens. J.*, vol. 12, no. 8, pp. 2711–2718, 2012.
- [3] S. Cheng and Z. Wu, "A microfluidic, reversibly stretchable, large-area wireless strain sensor," *Adv. Funct. Mater.*, vol. 21, no. 12, pp. 2282–2290, 2011.
- [4] Y.-L. Park, C. Majidi, R. Kramer, P. Bérard, and R. J. Wood, "Hyperelastic pressure sensing with a liquid-embedded elastomer," *J. Micromech. Microeng.*, vol. 20, no. 12, 2010.
- [5] R. D. P. Wong, J. D. Posner, and V. J. Santos, "Flexible microfluidic normal force sensor skin for tactile feedback," *Sens. Actuators, A*, vol. 179, pp. 62–69, 2012.
- [6] D. Vogt, Y.-L. Park, and R. J. Wood, "Design and characterization of a soft multi-axis force sensor using embedded microfluidic channels," *IEEE Sens. J.*, vol. 13, no. 10, pp. 4056–4064, 2013.
- [7] K. Noda, K. Matsumoto, and I. Shimoyama, "Stretchable tri-axis force sensor using conductive liquid," *Sens. Actuators, A*, vol. 215, pp. 123–129, 2014.
- [8] C. Majidi, R. Kramer, and R. J. Wood, "Non-differential elastomer curvature sensors for softer-than-skin electronics," *Smart Mater. Struct.*, vol. 20, 2011.
- [9] R. Kramer, C. Majidi, and R. J. Wood, "Wearable tactile keypad with stretchable artificial skin," in *Proc. IEEE Int. Conf. Rob. Autom.*, 2011, pp. 1103–1107.
- [10] Y. Menguc, Y.-L. Park, E. Martinez-Villalpando, P. Aubin, M. Zisook, L. Stirling, R. J. Wood, and C. J. Walsh, "Soft wearable motion sensing suit for lower limb biomechanics measurements," in *Proc. IEEE Int. Conf. Rob. Autom.*, 2013, pp. 5289–5296.
- [11] S. Cheng and Z. Wu, "Microfluidic stretchable RF electronics," *Lab Chip*, vol. 10, pp. 3227–3234, 2010.
- [12] F. L. H. III, R. K. Kramer, Q. Wan, R. D. Howe, and R. J. Wood, "Soft tactile sensor arrays for force feedback in micromanipulation," *IEEE Sens. J.*, vol. 14, no. 5, pp. 1443–1452, 2014.
- [13] A. Qusba, A. K. RamRakhyani, J.-H. So, G. J. Hayes, M. D. Dickey, and G. Lazzi, "On the design of microfluidic implant coil for flexible telemetry system," *IEEE Sens. J.*, vol. 14, no. 4, pp. 1074–1080, 2014.
- [14] Y.-L. Park, D. Tepayotl-Ramirez, R. J. Wood, and C. Majidi, "Influence of cross-sectional geometry on the sensitivity of liquid-phase electronic pressure sensors," *Appl. Phys. Lett.*, vol. 101, no. 19, 2012.
- [15] D. Tepayotl-Ramirez, T. Lu, Y.-L. Park, and C. Majidi, "Smart pneumatic artificial muscle actuator with embedded microfluidic sensing," *Appl. Phys. Lett.*, vol. 102, no. 4, 2013.
- [16] A. (6.13-3), "ABAQUS Documentation," in *Dessault Systems*, Providence, RI, 2011.